C. R. Mecanique 343 (2015) 397–409

Contents lists available at ScienceDirect

Comptes Rendus Mecanique

www.sciencedirect.com

A numerical and semi-analytical comparison for structural analysis of fault-crossing pipelines

Omar González, Alberto Fraile *, Lutz Hermanns

Centro de Modelado en Ingeniería Mecánica (CEMIM), Universidad Politécnica de Madrid (UPM), José Gutiérrez Abascal 2, 28006 Madrid, Spain

ARTICLE INFO

Article history:
Received 30 April 2015
Accepted 11 June 2015
Available online 3 July 2015

Keywords:
Pipeline
Earthquake
Finite element method
Nonlinear analysis
Fault
Design criteria

ABSTRACT

Structural analysis of pipelines is a well-established topic in engineering practice. Different professional societies or national and international authorities have provided Design Codes with procedures that, in spite of being well accepted, contain assumptions whose implications are not always well understood.

In this paper, we present a comparison between a simplified well-established method to compute the safety of gas pipes when crossing faults, and a more refined approach: the Finite Element Method (FEM) that enables us to consider large displacements and nonlinear material properties and shows some discrepancies relative to the classical approach.

1. Introduction

Pipelines related to industrial supplies such as oil or gas are a key part of modern development, so it is important to ensure their appropriate response to a seismic action. The same applies to drainage or water supply in contemporary cities.

Given its linear development over large geographic areas, a pipeline system crossing faults and other geologic features is unavoidable; therefore an important aspect of structural analysis is the evaluation of stresses and strains in the structure when crossing faults.

Although the study of buried pipelines started early (Reese et al. [1]), the first influential work on the subject was presented by Newmark and Hall [2]. They assumed that the flexibility of the pipe allows it to adapt to ground deformations, a condition that has remained throughout all subsequent studies. Under these conditions, the crossing of a fault scarp is especially critical. There is a discontinuity in the surrounding land topography that causes the pipe to distort to compensate for the fault offset, without damaging its functionality. However, the underlying assumption made by Newmark and Hall that the strain caused by axial forces dominates, i.e. local bending strain in the pipe is ignored, may result in underestimation of maximum strain.

Newmark himself [2] and later Kennedy et al. [3], Singhal [4], Trautmann et al. [5,6] Nyman et al. [7] proposed simplified alternatives that reduced checks to simple operations. These methods were systematized and popularized with the Guide by the American Society of Civil Engineers (ASCE) [8] that unified the procedures followed worldwide. The European Union has also proposed standards based on the same approach [9].

In some cases, however, questions have been raised about the actual precision of the simplified methods (see, for instance, Savidis et al. [10], Butenweg et al. [11]).

* Corresponding author. Tel.: +34 91 336 5346; fax: +34 91 336 5345.
E-mail address: alberto.fraile@upm.es (A. Fraile).

http://dx.doi.org/10.1016/j.crme.2015.06.003
1631-0721/

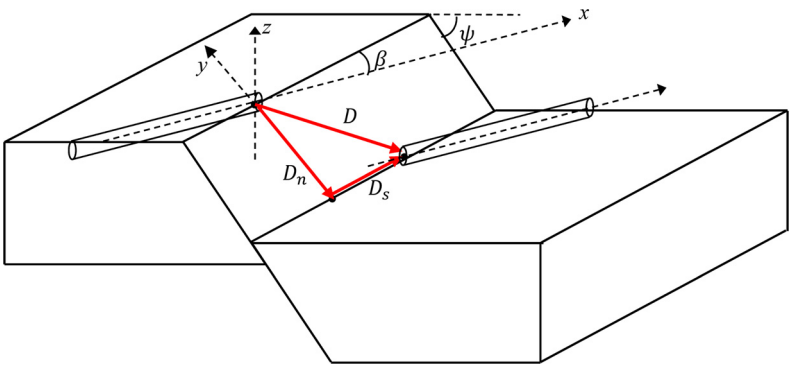

Fig. 1. (Color online.) Representation of the fault.

Therefore, in this paper, we have chosen to use the Finite Element Method (FEM) to check, with some particular examples, the results obtained by Kennedy's method [3]. These examples demonstrate the existence of some limitations to the actual accuracy of the results obtained with the simplified method.

1.1. Calculation methods

For buried steel pipelines, the most common approach to study their capacity is to use its deformability, either elastic or inelastic, to accommodate the soil distortions without failure. The pipeline alignment should be selected so that the duct is preferably subjected both to axial tensile and bending stresses, while the compressive stresses are kept to a minimum to prevent buckling from occurring. In fact, Kennedy's method is only valid for pipes under tension.

The fault movement is generally idealized as a plane discontinuity, characterized by the strike and the dip (Fig. 1) and the induced displacement components called strike-slip D_s and dip-slip D_n, respectively. To study the interaction between the duct and the fault, in addition to the dip angle ψ, we have to consider also the angle β between the pipe direction and the strike line.

In general, displacements induced by the fault will be three-dimensional and depend on the magnitude of strike and dip components. The three displacements D_x, D_y, and D_z in three perpendicular directions, x, y, and z, which vary with the crossing angle, β, and the dip angle, ψ, will have to be imposed on the FE model.

There are several methods for analyzing buried pipes when crossing faults. These methods could be generalized for similar concepts as drainage networks or water supply with appropriate modifications to the boundary conditions. This work analyzes only Kennedy's method, which is the most used in routine works as well as the FEM, which nowadays, because of current computers' capabilities, is also a practical design alternative.

1.1.1. Kennedy's method

Kennedy's method assumes that the pipe adapts to the fault movement with a deformation composed of two straight lines connected by a constant curvature part (Fig. 2, see Appendix A for meaning of variables). It is also assumed that there are two effective anchoring points (A and B_2), subjected to the same displacement as the neighboring soil.

This method considers soil lateral forces on the pipeline, the resulting curvature and stretching as well as the associated axial and bending stresses. (See Appendix A.)

To evaluate the interaction forces, soil mechanics background is necessary: bearing capacity, limit loads, earth pressures, longitudinal friction forces, etc., recognizing different values of frictional resistance along the straight and curved parts of the pipe (see Appendix B taken from reference [8]).

The method will result in an upper-bound estimate of strain, since bending strain is overestimated while assuming that the pipeline follows the soil masses as a hanging cable without any bending stiffness.

1.1.2. Finite Element Method (FEM)

Several authors [8–10] recommend the use of FEM in order to introduce a variety of soil properties, plasticity effects both in the duct and in the soil, as well as possible nonlinear geometric effects.

The duct is modeled using 3D beam elements with nonlinear properties. For the surrounding soil, several studies [10,12] have shown that there is no practical advantage in using a 3D soil model compared with those obtained using equivalent nonlinear springs, as recommended by reference [8].

The FEM permits to obtain displacements and strains for practically any number of points of interest, and the effects of a wide variety of parameters can be analyzed with relative ease.

The inelastic behavior of the pipe is simulated by specifying a nonlinear stress–strain curve for the pipe material. The stress–strain curve is generally piecewise linear to approximate the stress–strain law specific of the steel used, which in turn, is usually modeled by a Ramberg–Osgood law (Fig. 3).

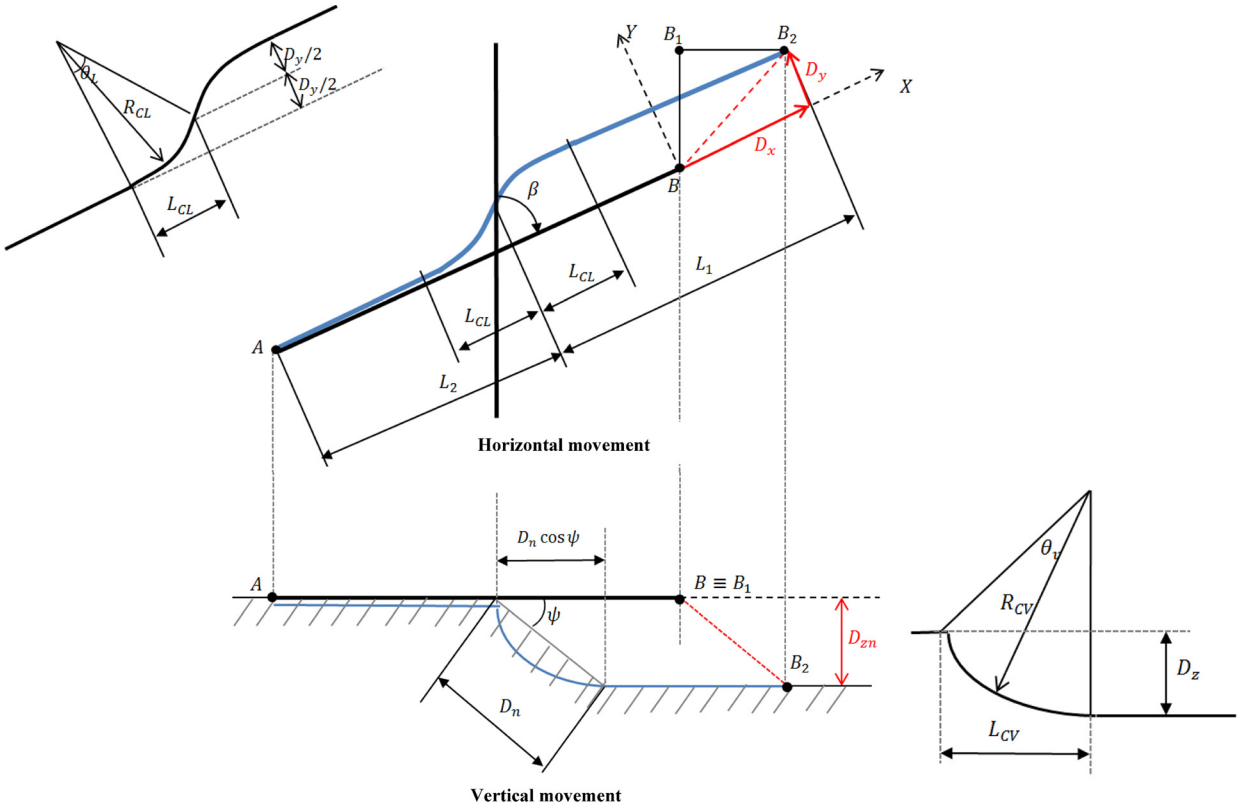

Fig. 2. (Color online.) Generic movement of the pipeline [8].

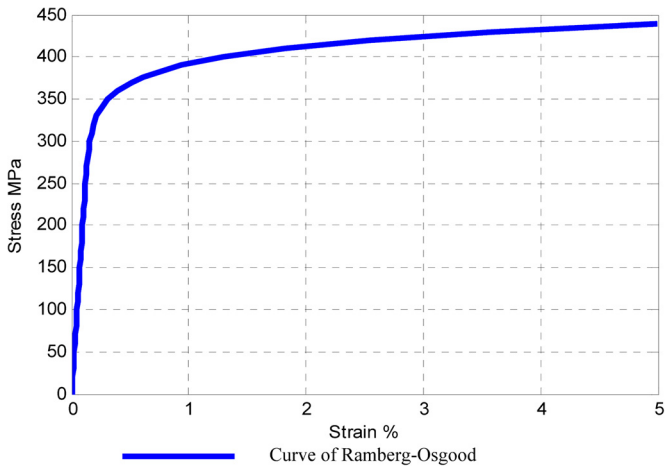

Fig. 3. (Color online.) Ramberg–Osgood stress–strain relation.

Obviously, the pipeline segment used in the model must be sufficiently long to adequately characterize the behavior at the fault location, i.e., it must extend beyond the fault to reach virtual anchor points at each side of it.

Soil–pipeline interaction is modeled by springs in three directions, one axial and two transverse (horizontal and vertical), which is schematically represented in Fig. 4.

The longitudinal springs represent restrictions on axial forces along the pipe wall reflecting the friction between the pipeline and the ground. Transverse springs are used to simulate the horizontal and vertical soil resistance perpendicular to the pipe axis. Although horizontally they are given the same stiffness, in the vertical plane we have to consider different stiffness curves to simulate the effects of downward or upward soil resistance (see Appendix B).

The force exerted on the pipeline is a nonlinear function of relative displacement of the soil-pipeline system. The material laws are indicated by soil reaction-displacement curves t–x, p–y, q–z, axial, transverse and vertical, respectively (Fig. 5).

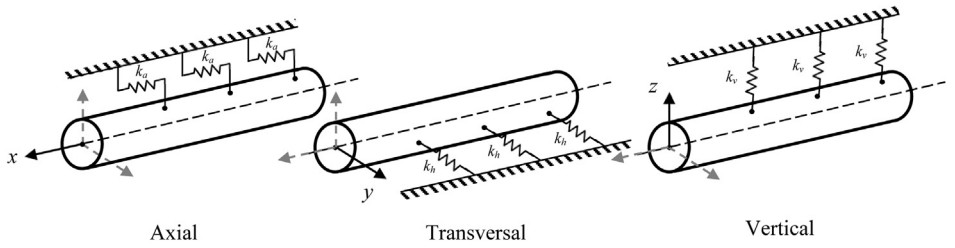

Fig. 4. Schematic representation of soil springs.

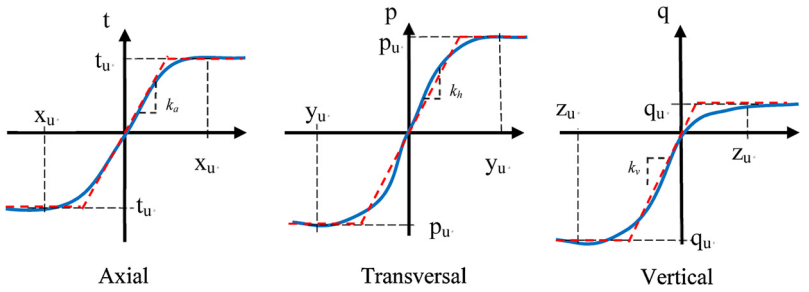

Fig. 5. (Color online.) Force-displacement curves of the soil springs.

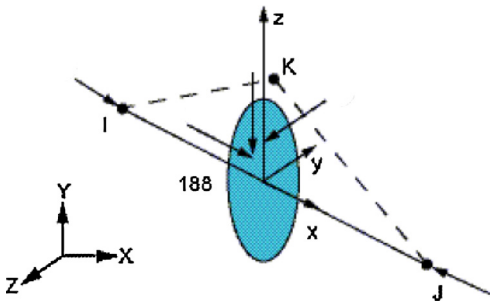

Fig. 6. (Color online.) Node locations and coordinate system of the beam element.

If large relative displacements (greater than x_u, y_u and z_u) of the connecting node with the pipeline occur, soil reactions reach a maximum constant value (t_u, p_u and q_u).

Fault displacement is introduced in the model as imposed displacements on the soil nodes. Beside other results of interest, nodal displacements, final axial forces and moments, longitudinal strains and stresses in the pipe wall are obtained. Nonlinear aspects of the problem are due to large displacements on the order of the pipe section, causing geometrically nonlinear effects as well as nonlinear material behavior in the soil springs.

The FEM equations can be assembled as usual

$$\mathbf{K} \cdot \mathbf{v} = \mathbf{F} \tag{1}$$

where the stiffness matrix $\mathbf{K}$ is the sum of the current value of $\mathbf{K}_{st}$, the pipeline stiffness, and $\mathbf{K}_s$, the current value of the soil spring stiffness values:

$$\mathbf{K} = \mathbf{K}_{st} + \mathbf{K}_s \tag{2}$$

On the other hand, $\mathbf{F}$ is the force vector induced by the difference between the structural degrees of freedom $\mathbf{v}$ and the imposed soil displacements $\mathbf{v}_s$, including the transverse and along-beam displacements if $\mathbf{v}$ represents the total displacement.

$$\mathbf{F} = \mathbf{K}_s \cdot \mathbf{v}_s \tag{3}$$

Due to the material's nonlinearities, we need to use an *iterative incremental approach*. On the other hand, as the displacements can reach values on the order of the duct diameter, a geometrically nonlinear formulation has to be used.

We have used the commercial code ANSYS for this purpose. The pipe is modeled with three-dimensional beam elements of type BEAM188, see Fig. 6. This type of element is appropriate for the analysis of moderately short slender beams and is based on the Timoshenko beam formulation. The element provides options to model a hollow tube section to simulate the behavior of the pipe.

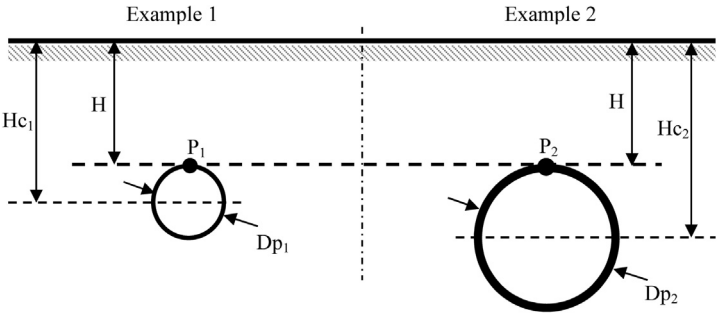

Fig. 7. Studied pipe configurations.

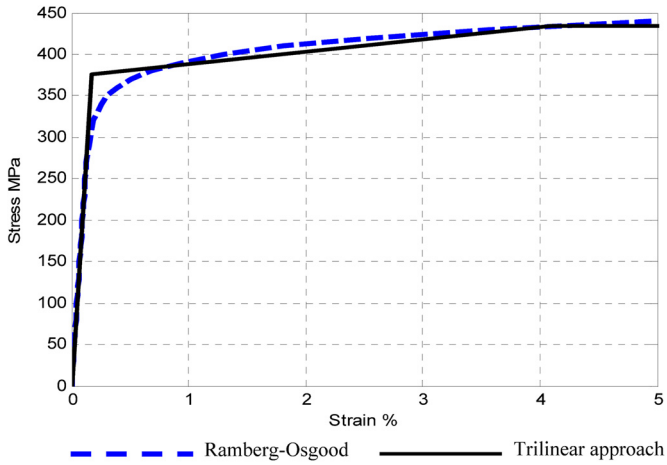

Fig. 8. (Color online.) Steel stress–strain diagram.

2. Case comparison

This section compares the results obtained using two pipes with different diameters. The objective is to check the differences that occur due to the simplifying assumptions used in Kennedy's method and to identify variables that significantly influence the response.

While varying the diameter of the pipe, we enforce the burial depth by maintaining the distance from the ground surface to the pipe top surface constant (Fig. 7). In this way, we change the uplift soil resistance as well as the bearing capacity both in the vertical and the horizontal directions.

The geometry of the two pipelines is defined by diameters of 0.3048 m (12 in) and 0.6096 m (24 in) and a wall thickness that is 2% of the respective diameter.

The burial depth is $H = 0.91$ m (3 ft).

The steel used is of grade X46 with a value of the elastic limit of 375 MPa and Ramberg–Osgood parameters $\alpha = 36.7$ and $r = 14.30$. A trilinear approach has been used in the FE model (Fig. 8).

The soil is considered to be dry sand, with a specific weight of 18 kN/m^3, an at-rest coefficient $K_0 = 0.5$ and an internal friction angle of 36°.

For its part, the fault-duct system is geometrically characterized by a normal fault with a dip angle $\psi = 75°$ and a crossing angle $\beta = 50°$. The strike slip is zero and the dip slip along the inclined fault surface has a value of 0.85 m.

As usual, it is assumed that the soil in the displacing fault side moves as a rigid body imposing three displacements along the x, y, and z axes, as shown in Fig. 1, whose values are $D_x = 0.1685$ m, $D_y = -0.1414$ m and $D_z = -0.8210$ m, respectively, for each direction.

The FEM model has a total length of 700 m. This length has been chosen as an initial value for a convergence study of the distance between the fault plane and the mesh boundaries.

The entire duct is discretized with 1-m-long elements, except for the central part of the pipe, 20 m on each side of the fault, where an element length of 0.1 m has been used to account for the high strain gradients in this region. This can be seen in Fig. 9.

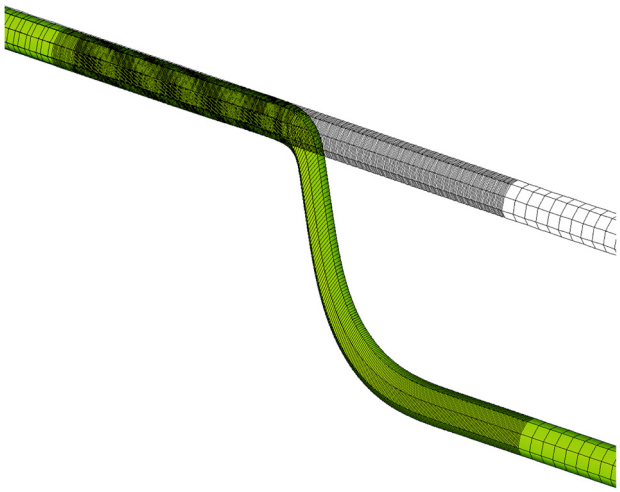

Fig. 9. (Color online.) Pipeline deformation (not to scale).

Table 1
Subgrade reaction.

Subgrade reaction		Example 1	Example 2	Units
Axial straight part	t_u	5.39	12.33	kN/m
Axial curved part	t_{uc}	17.66	32.24	kN/m
Transverse	p_u	77.56	148.17	kN/m
Vertical upward	q_u	16.43	22.34	kN/m
Vertical downward	q_u	251.49	633.05	kN/m
Axial relative displacement	x_u	0.25	0.58	cm
Transverse relative displacement	y_u	2.41	4.60	cm
Vertical upward relative displacement	z_u	1.05	1.43	cm
Vertical downward relative displacement	z_u	3.05	7.67	cm

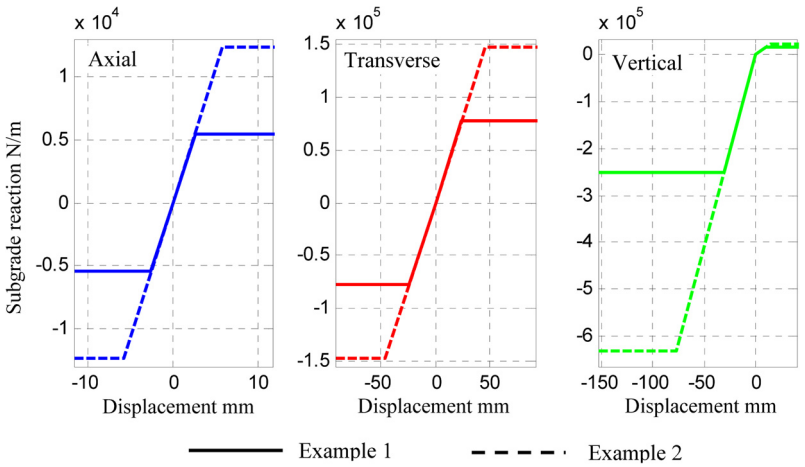

Fig. 10. (Color online.) Soil resistance for each example.

Soil mechanical characteristics and relative soil displacements are computed according to the formulation recommended by reference [8] and briefly described in Appendix B.

For the displacement of the larger diameter pipe (Example 2), we maintain the same stiffness ratio as in Example 1 (see Table 1 and Fig. 10).

2.1. Results

Using Kennedy's method, convergence of the axial stress in the pipe is reached when the geometric elongation and stress-induced stretching are equal.

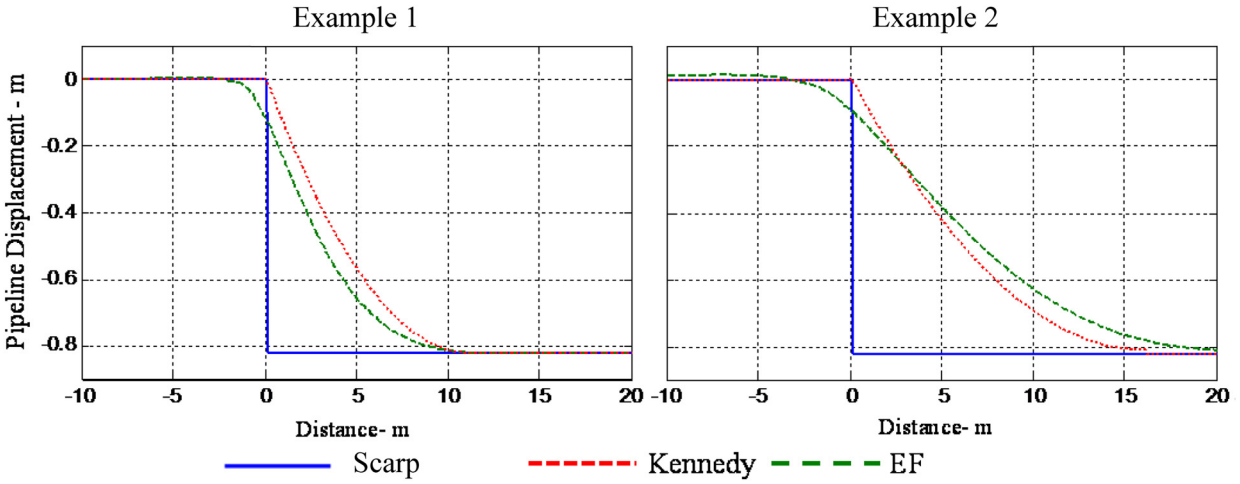

Fig. 11. (Color online.) Vertical pipeline displacement.

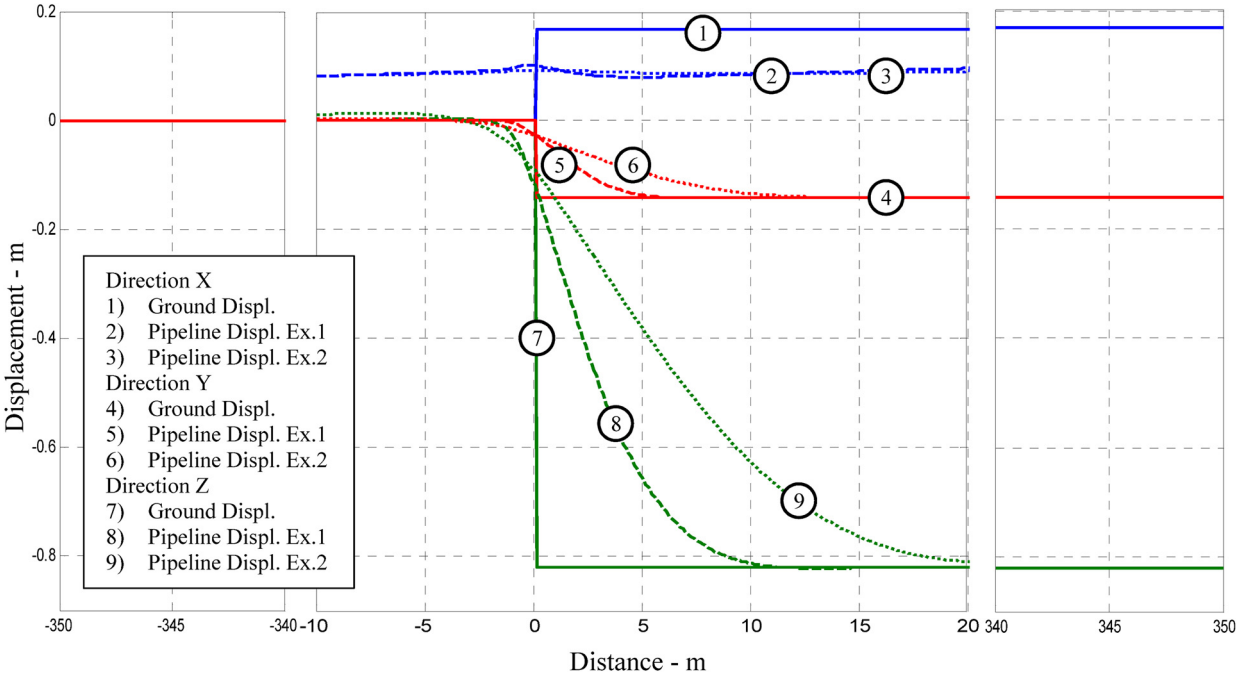

Fig. 12. (Color online.) Horizontal and vertical ground and pipeline displacements.

In this way, we obtained axial steel stresses $\sigma_a = 206.7$ MPa and $\sigma_a = 150.5$ MPa for diameters 12 and 24 inches, with elongations equal to 0.21 m and 0.20 m, respectively.

In our examples, the convergence values correspond to total strains (axial and bending) of 1.10% and 1.37%, respectively. We could see an increase in strain and a reduction in axial stress as larger pipe diameters were used due to the dependence of the constant pipe curvature on the soil stiffness.

In Fig. 11 the vertical displacements along the pipe axis are shown for both examples and in Fig. 12 all displacement components obtained by FE analysis are plotted. From both figures, it can be seen that the distance between the fault and the virtual anchoring points is larger in Example 2.

By increasing the pipe diameter, we generate also an increase in soil stiffness and resistances to uplift and bearing (Fig. 7) along with a simultaneous increase in the pipeline stiffness. The combined effects of these factors lead to a reduced strain.

The greatest concentration of stresses is generated in areas near the fault jump where the pipeline is subjected to higher bending and axial stresses. The strain components (axial and bending) for the upper point (P_1 and P_2 in Fig. 7) of the transverse cross-section can be seen in Fig. 13.

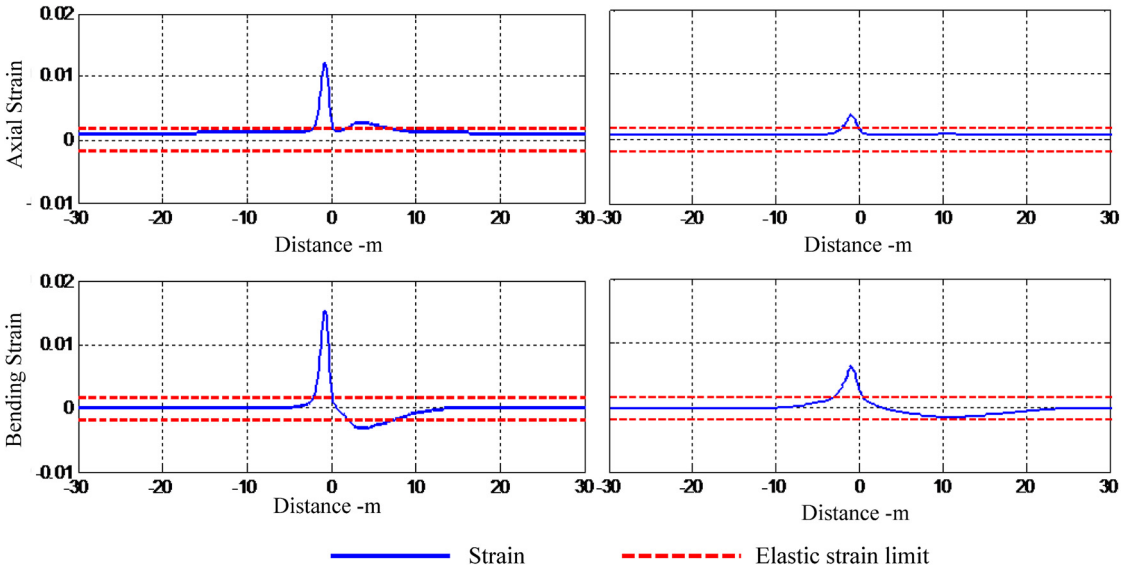

Fig. 13. (Color online.) Axial strain ($\varepsilon_{\mathrm{dir}}$) and bending strain ($\varepsilon_{\mathrm{BzT}}$).

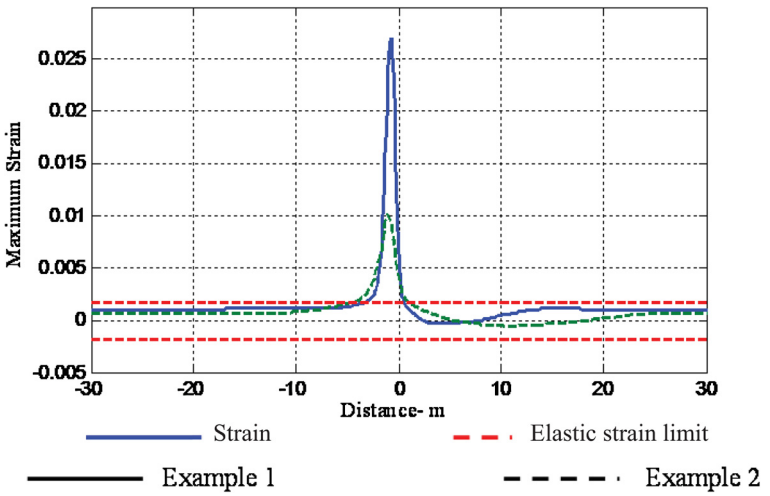

Fig. 14. (Color online.) Maximum strain distribution.

Positive values of strain are produced by the pipe axial stretching, where the geometric nonlinearity is very important, complemented by bending curvatures imposed by the ground onto the pipe.

The composition of the total strain as a sum of elastic and plastic strains, due to axial and bending effects, produce, for each of the examples, the results presented in Fig. 14 clearly showing the reduction in strain when increasing the diameter of the pipe.

The maximum strains obtained are 2.70% and 1.01%, respectively, for each one of the examples. (See Table 2.) They are developed very close to the fault's crossing section.

2.2. Conclusions from the comparison

The main difference between the results of the methods refers to the bending curvature (Fig. 13) and thus an analysis of the curvatures will be done following both methods for each example given.

In Kennedy's method (see Fig. 2), the pipe curvature is assumed to be constantly zero from the anchoring point in the upper fault block, until its very intersection with the upper border of the fault. From then on, the duct hangs with a constant curvature. Savidis [10] suggests that this may be thought of as if a plastic hinge had been formed up there.

The constant radius of curvature R in the hanging part can be estimated using the analogy of a membrane under uniform pressure p_{u}, where the axial force N is related to R by:

Table 2
Maximum strain values.

Strains [%]		Kennedy's method		Finite elements	
		Example 1	Example 2	Example 1	Example 2
Elastic strain	ε_{el}	–	–	0.20	0.186
Plastic strain	ε_{pl}	–	–	2.50	0.823
Axial strain	ε_{dir}	0.098	0.072	1.21	0.381
Bending strain	ε_{BzT}	1.00	1.30	1.53	0.647
Maximum Strain	$\varepsilon_{el} + \varepsilon_{pl}$	1.10	1.37	2.70	1.01

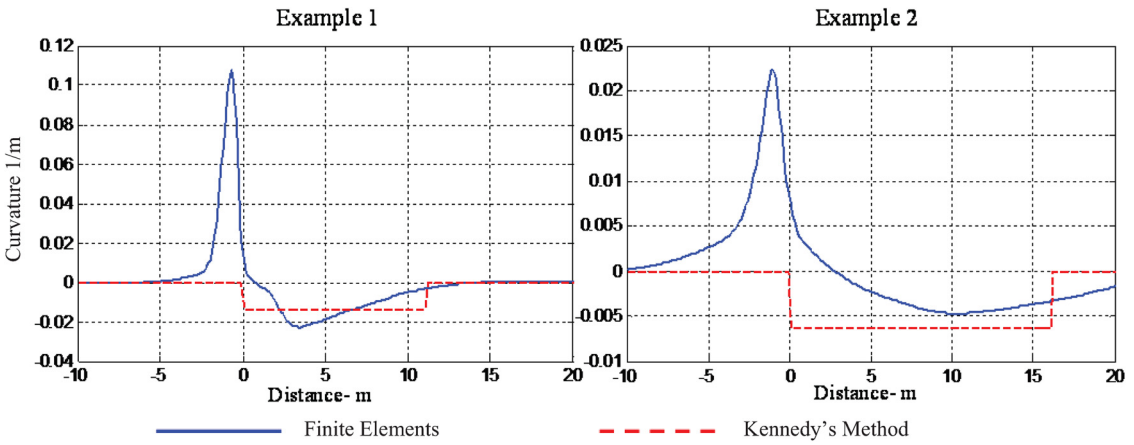

Fig. 15. (Color online.) Curvature comparison.

$$R = \frac{N}{p_u} \tag{4}$$

On its side, the curvature obtained by the FEM is deduced from the computed bending strains varying along the length as:

$$\chi_{EF} = \frac{2\varepsilon_{BzT}}{D_p} \tag{5}$$

In the examples studied, absolute maximum curvature values of 0.1007 m^{-1} and 0.02123 m^{-1}, respectively, are obtained for each of the cases that correspond with the border of the fixed part of the fault, precisely the point where Kennedy's method disregards the bending stiffness. Regarding Example 2 in Fig. 15, we can see that, as expected, Kennedy's estimated curvature is an upper bound in the hanging part, but it is not for the whole pipeline.

For smaller diameters, the strain obtained by FEM is larger than the one obtained with Kennedy's method because the maximum curvature is larger; the opposite occurs for larger diameters, implying that the increase in diameter reduces curvature, causing a reduction in strain.

3. Influence of the pipeline diameter

In order to quantify the differences obtained with Kennedy's method, we have performed calculations using different diameters and compared the maximum computed strains and curvatures in the pipe.

Regarding Kennedy's method, we have taken the constant curvature value that depends on the applied force and the soil stiffness, recalling that this implies that a plastic hinge in the upper border of the pipe will appear, precisely where the FEM shows the maximum strain values in the previous examples.

The bending strain evaluated through both methods is shown in Fig. 16. The FEM results show that by increasing the pipe diameter, the strain obtained at the highest point of the most demanded pipeline cross-section is considerably reduced, whereas with Kennedy's method the opposite effect is observed.

The comparison suggests that the use of Kennedy's method should be restricted to fault displacements approximately twice the diameter of the pipeline, since the biggest influence on the global strain comes from the bending strain.

This is supported by the good agreement between the results obtained for a fault movement of 0.85 m, which corresponds to 139% and 279% of the pipe diameters analyzed before.

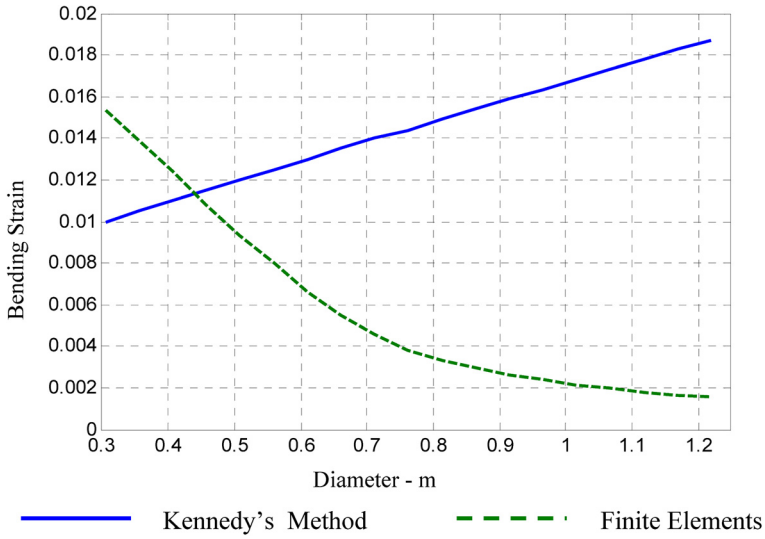

Fig. 16. (Color online.) Maximum bending strain as a function of pipe diameter.

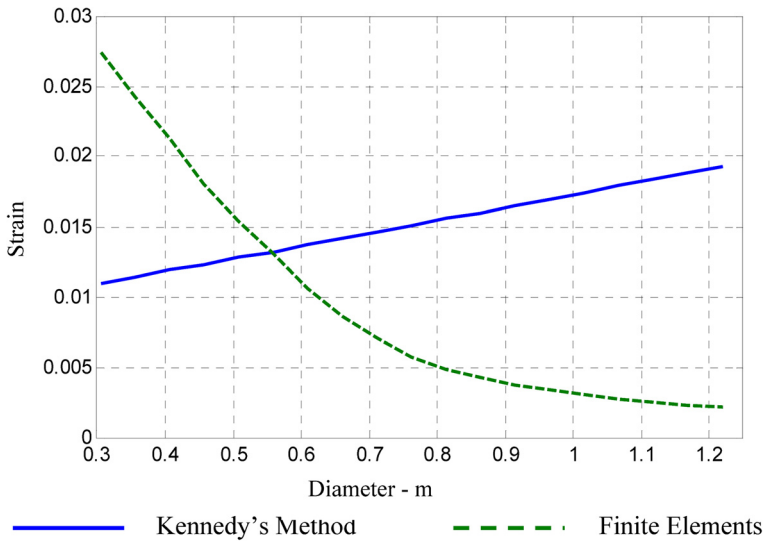

Fig. 17. (Color online.) Maximum strain as a function of pipe diameter.

Combining axial and bending strains, the results presented in Fig. 17 are obtained where larger differences are observed for smaller diameters, probably due to differences in bending contributions that rule over the associated stretching contributions.

The constant bending curvature postulated by Kennedy in the central part of the model and the maximum curvature at the most unfavorable point of the pipe obtained with the FE model are plotted against the pipe diameter in Fig. 18.

In comparison with the curvature values obtained by the FEM, the values corresponding to Kennedy's method are not conservative, especially for small pipe diameters.

4. Conclusions

The main objective of the paper is to draw the attention of the reader to the fact that Kennedy's method has to be used taking into account its limited area of application, which results from the assumptions the method is based on.

According to Kennedy's method, the curvature in the central part of the pipeline is constant. By increasing the pipe diameter and keeping the burial depth constant, the depth of the pipe axis increases. This increase results in higher soil resistance values and a different bending strain distribution along the pipe, as can be seen in Fig. 16.

According to the examples presented, an increase in pipe diameter results in a larger distance between the fault and the virtual anchoring points.

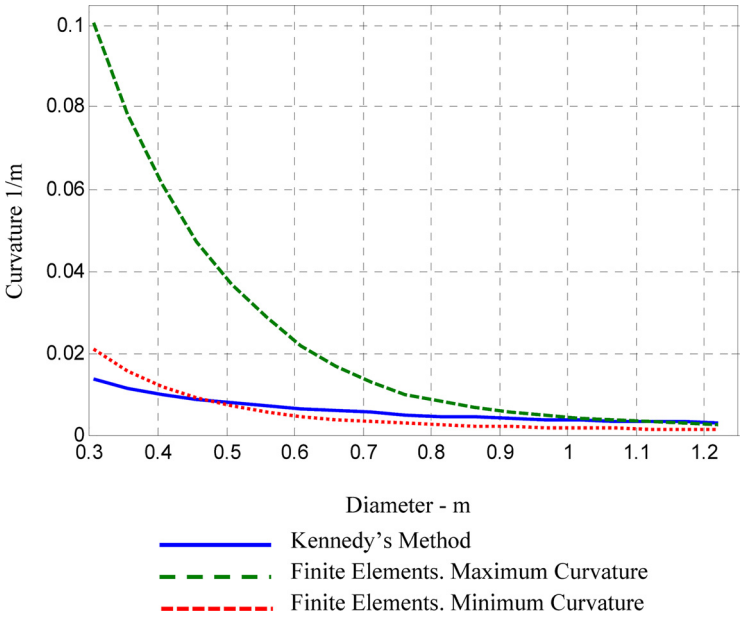

Fig. 18. (Color online.) Curvature comparison.

Comparing the values obtained for bending deformations by FE and Kennedy's method suggests that the results of the latter should be considered as an upper bound for curvatures only in cases where the fault displacement is on the order of twice the pipe diameter.

Probably the most influential factor in the differences obtained is related to the hypothesis that the strain remains constant in the pipe, which is not always a conservative assumption.

Finally, we should remember the significant influence of the steel grade on the deformation capacity of the pipeline because strain-based design involves comparing the strain demand resulting from the applied loads with the strain capacity that is affected by pipe geometry, material properties and defects due to fatigue or physical damage.

The first author would like to thank the Ministry of Education of the Dominican Republic for the scholarship provided for his studies of Master and Doctorate at the "Earthquake Engineering and Structural Dynamics Soil" program of the Universidad Politécnica of Madrid (UPM).

Appendix A. Kennedy's method

According to Kennedy's method, the moving part of the fault behaves as a rigid body forcing the pipeline to curve and to displace the surrounding soil in areas near fault zones.

The fault jump D is composed of a strike component D_s and a dip one D_n related through factor k_{DS}. (See Fig. 1.)

$$D_s = k_{DS} D \qquad D = \sqrt{D_s^2 + D_n^2} \tag{6}$$

Thus, by decomposing the total movement of the pipe in three perpendicular directions, x (collinear to the axis of the pipe), y (perpendicular to the axis and in the horizontal plane), and z (perpendicular to the previous two), D_x and D_y are produced both by strike and dip slips, and D_z only by dip slip (see Fig. 2).

The three components of the movement of the pipe are given by:

$$D_x = D_{xs} + D_{xn} = D\left[k_{DS}\cos\beta + \sqrt{1-k_{DS}^2}\cos\psi\sin\beta\right] \tag{7}$$

$$D_y = D_{ys} + D_{yn} = D\left[k_{DS}\sin\beta - \sqrt{1-k_{DS}^2}\cos\psi\cos\beta\right] \tag{8}$$

$$D_z = D\sqrt{1-k_{DS}^2}\sin\psi \tag{9}$$

The radii of curvature of the lateral and vertical movements (R_{cl} and R_{cv}, respectively) are considered constant throughout the curved region:

Table 3
Soil resistance values [8].

Component	Relationship for fully buried pipelines
Longitudinal (curve t–x)	$t_u = \begin{cases} \pi D \alpha S_u & \text{for clay} \\ \frac{\pi D}{2} \overline{\gamma} H_c (1 + K_0) \tan \emptyset & \text{for sand} \end{cases}$
	$x_u = \begin{cases} 0.1 \text{ to } 0.2 & \text{inches for dense to loose sand} \\ 0.2 \text{ to } 0.4 & \text{inches for stiff to soft clay} \end{cases}$
Transversal (curve p–y)	$p_u = \begin{cases} S_u N_{ch} D & \text{for clay} \\ \overline{\gamma} H_c N_{qh} D & \text{for sand} \end{cases}$
	$y_u = \begin{cases} 0.07 \text{ to } 0.10(H_c + D/2) & \text{for loose sand} \\ 0.03 \text{ to } 0.05(H_c + D/2) & \text{for medium sand} \\ 0.02 \text{ to } 0.03(H_c + D/2) & \text{for dense sand} \\ 0.03 \text{ to } 0.05(H_c + D/2) & \text{for stiff to soft clay} \end{cases}$
Vertical (curve q–z)	Upward direction:
	$q_u = \begin{cases} S_u N_{cv} D & \text{for clay} \\ \overline{\gamma} H_c N_{qv} D & \text{for sand} \end{cases}$
	$z_u = \begin{cases} 0.01 \text{ to } 0.015 H_c & \text{for dense to loose sand} \\ 0.1 \text{ to } 0.2 H_c & \text{for stiff to soft clay} \end{cases}$
	Downward direction:
	$q_u = \begin{cases} S_u N_c D & \text{for clay} \\ \overline{\gamma} H_c N_q D + \frac{1}{2} \gamma D^2 N_y & \text{for sand} \end{cases}$
	$z_u = 0.10 \text{ to } 0.15 D$ for both sand and clay

Nomenclature
S_u = Undrained shear strength of soil
α = Empirical coefficient that varies depending on S_u
$\overline{\gamma}$ = Effective unit weight of soil
D = External pipeline diameter
H_c = Depth from the ground surface to center of the pipeline
K_0 = Coefficient of soil pressure at rest
$\emptyset$ = Friction angle
N_{ch} and N_{qh} = Horizontal load capacity factor for cohesion and overload, respectively.
N_{cv} and N_{qv} = Vertical load capacity factor for cohesion and overload, respectively.
N_c, N_q, and N_y = Vertical capacity factor, cohesion, overload and friction, respectively.

$$R_{cl} = \frac{\sigma A_s C_p}{p_u} \tag{10}$$

$$R_{cv} = \frac{\sigma A_s C_p}{q_u} \tag{11}$$

where

A is the cross-section area of the pipeline,
σ is the normal stress,
C_p is the correction coefficient that considers the influence of the internal pressure,
p_u is the transversal soil resistance,
q_u is the vertical soil resistance,
R_{cl} is the lateral curved length,
R_{cv} is the vertical curved length,
D_n is the component of dip fault displacement,
D_v is the transversal component of displacement,
D_z is the vertical component of displacement.

Convergence of the method

The convergence of the method is reached when getting compatibility between the geometrical and tension-induced elongation of the pipe and the fault movement D, which is characterized by angles ψ and β.

The maximum tension is the parameter that is modified in the iterative process to equate the geometrical and tension-induced elongation of the pipe.

Appendix B. Soil resistance parameters

Soil resistance values that were collected from documents referred to by the ASCE and listed in [8] are compiled in Table 3.

References

[1] L.C. Reese, A.O.P. Casbarian, Pipe soil interaction for a buried offshore pipeline, Paper SPE 2343, presented at the 43rd Annual Fall Meeting of Society of Petroleum Engineers of AIME, TX, USA, 1968.
[2] N.M. Newmark, W.J. Hall, Pipeline design to resist large fault displacement, in: Proceedings, U.S. National Conference on Earthquake Engineering, Ann Arbor, MI, EERI, 1975.
[3] R.P. Kennedy, A.W. Chow, R.A. Williamson, Fault movement effects on buried oil pipeline, J. Transp. Eng.-ASCE 103 (TE5) (1977) 617–633.
[4] A.C. Singhal, Strength characteristic of buried jointed pipelines, Report to The Engineering Foundation and ASCE, Grant No. RC-A-77-6A, 1980.
[5] C.H. Trautmann, T.D. O'Rourke, Behavior of pipe in dry sand under lateral and uplift loading, Geotechnical Engineering Report 83-6, Cornell University, Ithaca, NY, 1983.

[6] C.H. Trautmann, T.D. O'Rourke, Load-displacement characteristics of pipe affected by permanent earthquake ground movements, in: Proceedings of the International Symposium on Lifeline Earthquake Engineering, PVP-77, Portland, OR, USA, ASME, 1983, pp. 254–262.
[7] D.J. Nyman, Guidelines for the Seismic Design of Oil and Gas Pipeline Systems, ASCE, New York, 1984, pp. 150–228.
[8] Guidelines for the Seismic Design of Oil and Gas Pipeline Systems, ASCE, 1984.
[9] EN 1594:2000. Gas supply systems – functional requirements.
[10] S. Savidis, W. Schepers, E. Nomikos, G. Papadakos, Design of natural gas pipeline subjected to permanent ground deformation at normal faults, in: 5th ICEGE, Santiago de Chile, 2011.
[11] C. Butenweg, T. Schmitt, B. Rosen, Seismische Einwirkungen auf erdverlegte Rohrleitungssysteme, Bauingenieur: die richtungsweisende Zeitschrift im Bauingenieurswesen 89 (7) (2014) 316–324.
[12] R. Winston Revie, Oil and Gas Pipelines: Integrity and Safety Handbook, Wiley–Blackwell, ISBN 978-1118216712, 2015.